Exciton versus Free Carrier Photogeneration in Organometal Trihalide Perovskites Probed by Broadband Ultrafast Polarization Memory Dynamics

ChuanXiang Sheng, Chuang Zhang, Yaxin Zhai, Kamil Mielczarek, Weiwei Wang, Wanli Ma, Anvar Zakhidov, and Z. Valy Vardeny

Phys. Rev. Lett. **114**, 116601 — Published 18 March 2015

DOI: 10.1103/PhysRevLett.114.116601

Excitons versus Free Carriers Photogeneration in Organometal Trihalide Perovskites Probed by Broadband Ultrafast Polarization Memory Dynamics

ChuanXiang Sheng[1]*, Chuang Zhang[1], Yaxin Zhai[1], Kamil Mielczarek[2], Weiwei Wang[3], Wanli Ma[3], Anvar Zakhidov[2], and Z. Valy Vardeny[1]**

[1]*Department of Physics and Astronomy, University of Utah, 115 South 1400 East, Salt Lake City, Utah 84112, USA*

[2]*Department of Physics, University of Texas at Dallas, Richardson, Texas 75080, USA*

[3]*Institute of Functional Nano & Soft Materials (FUNSOM), Soochow University, Suzhou 215123, China*

We studied the ultrafast transient response of photoexcitations in two hybrid organic-inorganic perovskite films used for high efficiency photovoltaic cells, namely $CH_3NH_3PbI_3$ and $CH_3NH_3PbI_{1.1}Br_{1.9}$ using polarized broadband pump-probe spectroscopy in the spectral range of 0.3-2.7 eV with 300 fs time resolution. For $CH_3NH_3PbI_3$ with above-gap excitation we found both photogenerated carriers and excitons; but only carriers are photogenerated with below-gap excitation. In contrast, mainly excitons are photogenerated in $CH_3NH_3PbI_{1.1}Br_{1.9}$. Surprisingly, we also discovered in $CH_3NH_3PbI_3$, but not in $CH_3NH_3PbI_{1.1}Br_{1.9}$, transient photoinduced polarization memory for both excitons and photocarriers, which is also reflected in the steady state photoluminescence. From the polarization memory dynamics we obtained the excitons diffusion constant in $CH_3NH_3PbI_3$, $D \approx 0.01$ cm^2sec^{-1}.

* Permanent Address: School of Electronic and Optical Engineering, Nanjing University of Science and Technology, Nanjing, Jiangsu, 210094, China

** Author to whom correspondence should be addressed; e-mail: val@physics.utah.edu

The hybrid organic-inorganic photovoltaic (PV) solar cells based on the semiconductor class of methyl-ammonium (CH_3NH_3; MA) lead halide perovskites, $MAPbX_3$ (where X stands for halogen) have recently emerged as one of the most promising contenders, with extraordinary power conversion efficiencies up to an astonishing 19.3% [1-6]. The replacement of the inorganic cation in traditional perovskites by the isoelectronic MA^+ provides a unique way of tuning the chemical bonding and consequently also the optical and electronic response of these materials, which are therefore very different from those of the inorganic counterparts [7]. In particular, the exciton binding energy, E_B of typical hybrid perovskites such as $MAPbI_3$ and $MAPbBr_3$ has been reported to be in the range of 20-150 meV [8-10]; this is of the order of the thermal energy at room-temperature (k_BT = 26 meV at T = 300K). This intermediate E_B value bears upon one of the fundamental questions of the perovskites photophysics, namely the *branching ratio* between the photogeneration of free carriers and excitons. This is a crucial issue in that determines the PV efficiency of these materials. However a firm method to optically discern between these two kinds of photoexcitation species is still lacking [11-14], and thus the photogeneration of free carrier vs. exciton could not be reliably addressed so far.

In this work we studied the room-temperature ultrafast transient response of photoexcitations in two types of perovskite thin films, namely $MAPbI_3$ and $MAPbI_{3-x}Br_x$ with x=1.9, using the polarized pump-probe photomodulation (PM) spectroscopy in a *broad spectral range* from mid-IR to visible (0.3-2.7 eV) with 300 fs time resolution. We demonstrate the existence of *exciton/carrier duality* response in these hybrid perovskites. With above-gap pulse excitation we found in $MAPbI_3$ instantaneously generated carriers *and* excitons, but only carriers are photogenerated when excited below the gap (i.e. into the film's Urbach absorption tail). In $MAPbI_{3-x}Br_x$, however we detected mainly photogenerated excitons. Our results show that broadband ultrafast optical probe is *crucial* for revealing the characteristic perovskites photophysics properties, because photogenerated carriers and excitons in these materials contribute in different spectral ranges. Surprisingly, we found transient photoinduced polarization memory (POM) for both excitons and photocarriers characteristic photoinduced absorption (PA) bands in $MAPbI_3$ that is also reflected in the steady state photoluminescence (PL); it originates from the tetragonal crystal anisotropy of this perovskite at ambient conditions.

From the POM decay dynamics and the nano-crystallites size distribution in the $MAPbI_3$ film, we estimate the exciton diffusion constant in this perovskite to be D=0.01 cm^2/sec.

We used two laser systems based on Ti:Sapphire oscillator. These are: a low power (energy/pulse ~0.1 nJ) high repetition rate (~80 MHz) laser for the mid-IR spectral range; and a high power (energy/pulse ~10 μJ) low repetition rate (~1 kHz) laser for the near-IR/visible spectral range. The pump excitation for both laser systems was set at $\hbar\omega$ = 3.1 eV, which is above the optical gap of the two studied perovskites, or at $\hbar\omega$=1.55 eV which is below-gap excitation. For the low intensity measurements we used an optical parametric oscillator (Opal, Spectral-Physics) that generates $\hbar\omega$(probe) from 0.3 to 1.05 eV. Whereas for the high intensity measurements, white light super-continuum was generated for $\hbar\omega$ (probe) ranging from 1.15 to 2.7 eV. The transient PM spectra from the two laser systems were normalized to each other using the fundamental (1.55 eV) probe from the low power laser system. The PM spectrum contains photoinduced absorption (PA) bands with $\Delta T < 0$ due to excited state absorption; and photoinduced bleaching (PB) with $\Delta T>0$ caused by pump-induced bleaching of the ground state absorption, where ΔT is the change of the film transmission, T. For the transient POM study we measured ΔT(t) where the pump/probe polarizations were parallel or perpendicular to each other.

For growing the $CH_3NH_3PbI_3$ ($CH_3NH_3PbI_{3-x}Br_x$) films, CH_3NH_3I at 0.4g and PbI_2 at 1.16g ($PbBr_2$ at 0.92g) (the Mole ratio in both compounds are ~1:1) were mixed in anhydrous N,N-Dimethylformamide (2 ml) and allowed to stir overnight at 60°C. The precursor solution was then spin coated on cleaned sapphire substrate at 1000 RPM and annealed at ~100°C for 10 minutes. All processes were done in a glove-box filled with nitrogen (O_2 and H_2O < 1 ppm).

Figure 1 summarizes the ps transient PM spectroscopy results of the $MAPbI_3$ film with above-gap excitation. At t=0 the PM spectrum contains three main spectral features (Fig. 1(a)). In the visible/near-IR range there is a large PB band at ~1.65 eV which is correlated to a neighboring PA band (PA_2) that extends to higher energies. PB and PA_2 bands have been recently observed in the ps and nanosecond time domain, as well as in continuous-wave (cw) PM spectroscopy [3, 13-16]. It has been accepted that these bands are due to band-filling effect caused by the photocarriers in $MAPbI_3$ [3, 13-17]. The third feature in the transient PM spectrum is a PA band

in the mid-IR spectral range that peaks at ~0.8 eV (PA_1; Fig. 1(a)). To the best of our knowledge PA_1 is observed here for the first time in perovskite films. In Fig. 1(b) PA_1 decay dynamics is compared to that of PB at comparable pump intensity, where the respective dynamics is independent with the pump intensities. It is clearly seen that their decay dynamics are very different from each other, indicating that these two bands originate from *two different photoexcitations*. In agreement with this interpretation we also observed (Fig. 1(b) inset) a delay of ~1 ps at the onset of PB transient, which is not seen in $PA_1(t)$ dynamics. We therefore conclude that PA_1 is generated instantaneously, whereas PB generation is delayed.. We therefore conclude that PA_1 and PB/PA_2 features originate from two different species, suggesting the coexistence of two types of primary photoexcitations in this perovskite.

Being a band-like transition, PA_1 cannot be explained as due to free carriers that are thermalized in the continuum bands, and therefore have limited $\boldsymbol{k}$-value in the Brillouin zone; such photocarriers would show a Drude-like free carrier PA ($\sim\omega^{-2}$) rather than a PA band. We therefore assign PA_1 as due to photogenerated *excitons* (see detailed discussion in the suppl. info. (S.I.) [18] section S1 and Fig. S1); in contrast we identify the PA_2/PB feature as originating from photogenerated carriers. We now understand the delayed formation of PB as due to the relatively weak hot plasma thermalization rate by emitting LO phonons via the weak Froehlich interaction [16, 27]. We note that there are two clear exciton transitions in $MAPbI_3$ absorption spectrum, namely E_1 at 1.66 eV and E_2 at 2.48 eV (Fig. 1(a) inset) [10]. These two transitions are separated by ~0.8 eV, which indicates that PA_1 may be an optical transition from E_1 to E_2, similar to the transient PM spectrum in nanotubes [28]. In fact from band structure calculation that includes e-h interaction [10] the allowed high-energy exciton (Γ_4) is accompanied by a close forbidden exciton (Γ_3 and Γ_5) of which transitions from the lower lying exciton (Γ_4) are allowed. Fig. 1(b) shows that PA_1 decays as a power law $(t/t_0)^{-\alpha}$, where α ~0.21. This non-exponential decay originates from the exciton ensemble inhomogeneity in the disordered perovskite film. It may originate either from dispersive transport type process [29], where the exciton diffusion coefficient towards the recombination centers is time dependent [30], or a distribution $g(\tau)$ of lifetimes, τ [31] having a tail towards longer lifetimes of the form $[\tau/\tau_0]^{-(1+\alpha)}$.

Surprisingly, we also observed transient photoinduced dichroism for PA_1 (Fig. 2(a)), namely $\Delta T_{\|}$

$\neq \Delta T_{\perp}$, where $\Delta T_{\parallel}$ ($\Delta T_{\perp}$) is PA for the pump-probe polarizations parallel (perpendicular) to each other. The degree, P(t) of 'linear polarization memory', POM (Fig. 2(a)) at time t, is defined as $P(t) = (\Delta T_{\parallel} - \Delta T_{\perp})/(\Delta T_{\parallel} + \Delta T_{\perp})$. For PA_1, P at t=0, [namely $P(0)$] is relatively small, $P(0) \approx 0.11$; but is clearly observable. The obtained photoinduced dichroism indicates an anisotropic crystal structure, which is consistent with the tetragonal lattice structure of $MAPbI_3$ at ambient [32]. In order to best display the physics associated with the POM dynamics, we calculated P(t) from the decays of $\Delta T_{\parallel}(t)$ and $\Delta T_{\perp}(t)$, after fitting their respective decay dynamics using a power law form (see Fig. 2(a)).We define the POM lifetime,τ(POM) as the time for P(t) to decay to $P(0)/3$ value; consequently we find that $\tau(POM) \approx 150$ps for PA_1 (Fig. 2(a)).

For analyzing the POM dynamic decay we assume that the excitons are generated in a crystalline disk with equal probability across its surface, which subsequently reach the closest disk boundary in a diffusive motion. Consequently we may extract the exciton diffusion constant by assuming that the excitons lose their POM when they cross the grain boundary. From the scanning electronic microscopy (SEM) image, we estimate the average grain size in our perovskites film to be about 82 ± 27 nm (see S.I. [18] Figs. S2 and S3). Based on these assumptions we calculate P(t) decay lifetime $t_0=R^2/12D$, where D is the exciton diffusion constant and R is the average disk radius (see S.I. [18]). From $\tau(POM) \approx 150$ps and R = 41 nm we obtain $D = 0.01 \pm 0.005$ cm^2/sec, which is very close to D estimated by another technique [16].

We also found transient photoinduced POM for the PB band in the visible range (Fig. 2(b)). In contrast to PA_1, POM of PB is *negative* (namely $\Delta T_{\parallel} < \Delta T_{\perp}$), and much longer-lived. In addition, POM initial value for the PB, $P(0)= -0.04$ is much smaller than that of PA_1 ($P(0)=0.11$). The different POM properties obtained for PA_1 and PB again shows that these two bands do not originate from the same photoexcitation species. In this case the much slower P(t) decay for PB indicates that free carriers do not easily cross the boundary between neighboring crystalline grains, suggesting that grain boundaries are one factor that may influence charge mobility in the perovskites [33].

We also measured the polarization properties of the cw PL emission in $MAPbI_3$ at ambient that

was excited by a linearly polarized cw pump beam from an Ar^+ laser at 488 nm. The PL emission passed through a polarizer followed by a polarization scrambler, and was measured with polarization parallel, $PL_{\|}$ and perpendicular, $PL_{\perp}$ to the polarization of the pump beam. Figure 2(b) inset shows the spectrum of the two PL components and the PL polarization memory, P_{PL} defined by the relation: $P_{PL} = (PL_{\|} - PL_{\perp})/(PL_{\|} + PL_{\perp})$. It is clearly seen that the PL emission is polarized; in fact P_{PL} remains approximately constant at P_{PL}~-0.035±0.005 across the entire PL spectrum. In addition we also measured the polarization degree, P_{BB} of the emission from a blackbody radiator (BR) at the sample position, where $P_{BB} = (BB_{\|} - BB_{\perp})/(BB_{\|} + BB_{\perp})$, and $BB_{\|}(BB_{\perp})$ have the same meaning as $PL_{\|}(PL_{\perp})$ above. We found that $P_{BB}<0.007$ (see Fig. 2(b) inset), much smaller than P_{PL}. The rather surprising POM result for the cw PL emission from the perovskite film shows that PL originates from the optical transition at the band-edge. This is consistent with the PL spectrum which peaks at 780 nm (or 1.6 eV), very close to the PB band in the transient PM spectrum (Fig. 2(b)).

In Fig. 3(a) we show the transient PM spectrum of $MAPbI_3$ with below-gap excitation, ω_{pump}=1.55 eV, which is absorbed in the film's Urbach edge [34]. One possibility for the pump excitation in this case is an optical transition from the valence band (VB) edge to the conduction band (CB) tail inside the gap (the other possibility is symmetrically from the VB tail to the CB edge). Under these conditions exciton photogeneration is impossible, since $\omega_{pump} < E_1$~1.66 eV. Indeed no PA band in the mid-IR is observed (Fig. 3(a)), *and this justifies our assignment of PA_1 band as due to excitons*. In contrast the PB/PA_2 feature at the band edge is clearly seen, and the overall PM spectrum shows the same dynamics across the entire measured spectral range (see S.I. [18], Fig. S4). This is consistent with our interpretation that the PB/PA_2 feature is due to photogenerated carriers, since excitons are lacking here. Another interesting phenomenon is that the abnormal transient photoinduced POM is also obtained using below-gap excitation (S.I. [18], Fig. S4 inset).

We extended our transient spectroscopy measurements to another type of perovskites film, namely $MAPbI_{3-x}Br_x$. This perovskite might be important for tandem solar cell, because its optical gap can be tuned from ~1.7 eV to ~2.3 eV when the composition parameter, x changes from x=0 to 3. From the absorption edge of this film at ~2.1 eV (Fig. 3(b) inset), we estimate

x=1.9 for our film [23]. Figure 3(b) presents the transient PM spectrum of the $MAPbI_{1.1}Br_{1.9}$ film at t = 0 ps. Similar to the PM spectrum of $MAPbI_3$ shown in Fig. 1(a), the PM spectrum here also contains three features: PA_1 at ~0.5 eV, and PB and PA_2 at ~2.1 eV and 2.3 eV, respectively. We attribute PA_1 to interband exciton transition, similar to the analysis of this band in $MAPbI_3$. From the absorption spectrum (Fig. 3(b) inset) we identify two exciton transitions, E_1 at 2.1 eV and a broader transition, E_2 with a shoulder at 2.7 eV. Thus there is a possible interband exciton transition from E_1 to E_2. In contrast to $MAPbI_3$, the dynamics of all three PM bands up to 500 ps are the same this also includes their dynamics close to t=0. This shows that excitons may also generate PB band due to 'phase space filling' which modulates the film absorption edge in the form of the PB/PA_2 optical feature [35, 36]. We conclude that *excitons* are the primary photoexcitations in $MAPbI_{1.1}Br_{1.9}$. This is consistent with the larger exciton binding energy of this perovskite, which we estimate to be ~110 meV (S.I. [18], section S4). This is much larger than k_BT at ambient, thus preventing thermal dissociation of exciton to free carriers.

We also checked the existence of transient POM in this film at both PA_1 and PB bands (S.I. [18], section S5, Fig. S5). Unlike the photoinduced POM obtained in $MAPbI_3$, there is none observed in this film. This is consistent with the *isotropic* cubic crystal structure of this perovskite at ambient [23]. We note that the null result for the POM in $MAPbI_{1.1}Br_{1.9}$ actually validates the observed polarization memory for the photoexcitations in $MAPbI_3$.

In conclusion, we identified transient PA bands in the mid-IR range that are due to photogenerated excitons in both $MAPbI_3$ and $MAPbI_{1.1}Br_{1.9}$; this helps assessing the photogenerated branching ratio of carrier/excitons in these materials For $MAPbI_3$ both excitons and free carriers are photogenerated at short time with an estimated ratio of ~1:10, exposing that photocarriers dominate the photoexcitations in neat perovskites having relatively small exciton binding energy. In contrast, mainly excitons are photogenerated in $MAPbI_{1.1}Br_{1.9}$ at our pumping levels, due to the substantially larger exciton binding energy of this perovskite. The ambient crystal structure anisotropy in $MAPbI_3$ allows for photoinduced transient and cw polarization memory. We used this effect to estimate the exciton diffusion constant in this perovskite. Our results are validated since $MAPbI_{1.1}Br_{1.9}$ that is isotropic at ambient, does not show any transient polarization memory.

The work at the University of Utah was supported by the AFOSR through a MURI grant RA 9550-14-1-0037 (ps transient spectroscopy) and the DOE grant No. DE-FG02-04ER46109 (cw spectroscopy). At UT Dallas the work was supported by the Welch Foundation grant AT-1617.

References

[1] H. J. Snaith, J. Phys. Chem. Lett. **4**, 3623 (2013).
[2] A. Kojima, K. Teshima, Y. Shirai, and T. Miyasaka, J. Am. Chem. Soc. **131**, 6050 (2009).
[3] H.-S. Kim *et al*., Sci. Rep. **2**, 591 (2012).
[4] M. M. Lee, J. Teuscher, T. Miyasaka, T. N. Murakami, and H. J. Snaith, Science **338**, 643 (2012).
[5] J. Burschka, N. Pellet, S.-J. Moon, R. Humphry-Baker, P. Gao, M. K. Nazeeruddin, and M. Grätzel, Nature **499**, 316 (2013).
[6] H. Zhou *et al.*, Science **345**, 542 (2014).
[7] C. C. Stoumpos, C. D. Malliakas, and M. G. Kanatzidis, Inorg. Chem. **52**, 9019 (2013).
[8] S. Sun, T. Salim, N. Mathews, M. Duchamp, C. Boothroyd, G. Xing, T. C. Sumbce, and Y. M. Lam, Energy Environ. Sci. **7**, 399 (2014).
[9] M. Hirasawa, T. Ishihara, T. Goto, K. Uchida, and N. Miura, Physica B **201**, 427 (1994).
[10] K. Tanaka, T. Takahashi, T. Ban, T. Kondo, K. Uchida, and N. Miura, Solid State Commun. **127**, 619 (2003).
[11] M. Saba *et al*., Nat. Commun. **5**, 5049 (2014).
[12] V. D'Innocenzo, G. Grancini, M. J. P. Alcocer, A. R. S. Kandada, S. D. Stranks, M. M. Lee, G. Lanzani, H. J. Snaith, and A. Petrozza, Nat. Commun. **5**, 3586 (2014).
[13] F. Deschler *et al*., J. Phys. Chem. Lett. **5**, 1421 (2014).
[14] A. Marchioro, J. Teuscher, D. Friedrich, M. Kunst, R. van de Krol, T. Moehl, M. Grätzel, and J.-E. Moser, Nat. Photon. **8**, 250 (2014).
[15] S. D. Stranks , G. E. Eperon, G. Grancini, C. Menelaou, M. J. P. Alcocer, T. Leijtens, L. M. Herz, A. Petrozza, H. J. Snaith, Science **342**, 341 (2013).
[16] G. Xing, N. Mathews, S. Sun, S. S. Lim, Y. M. Lam, M. Grätzel, S. Mhaisalkar, and T. C. Sum, Science **342**, 344 (2013).
[17] J. S. Manser and P. V. Kamat, Nat. Photon. **8**, 737 (2014).
[18] See Supplemental Material at http://link.aps.org/supplemental/xxx, which includes Figures S1-S5 and refs. [7-10, 19-26].
[19] J. I. Pankove, Optical Processes in Semiconductors, Dover, New York, 1971.
[20] C. X. Sheng, Z. V. Vardeny, A. B. Dalton, and R. H. Baughman, Phys. Rev. B **71**, 125427 (2005).
[21] C. X. Sheng, M. Tong, S. Singh, and Z. V. Vardeny, Phys. Rev. B **75**, 085206 (2007).
[22] R. A. Kaindl, M. A. Carnahan, D. Hägele, R. Lövenich, and D. S. Chemla, Nature **423**, 734 (2003).
[23] J. H. Noh, S. H. Im, J. H. Heo, T. N. Mandal, and S. I. Seok, Nano Lett. **13**, 1764 (2013).
[24] N. Kitazawa, Y. Watanabe, and Y. Nakamura, J. Mater. Sci. **37**, 3585 (2002).
[25] I. B. Koutselas, L. Ducasse, and G. C. Papavassiliou, J. Phys.: Condens. Matter **8**, 1217

(1996).
[26] B. Streetman and S. Banerjee, Solid State Electronic Devices (6th Edition) Prentice Hall (2005).
[27] C. S. Ponseca, Jr. *et al.* J. Am. Chem. Soc. **136**, 5189 (2014).
[28] O. J. Korovyanko, C. X. Sheng, Z. V. Vardeny, A. B. Dalton, and R. H. Baughman, Phys. Rev. Lett. **92**, 017403 (2004).
[29] Z. V. Vardeny and J. Tauc, Semiconductors Probed by Ultrafast Laser spectroscopy, R. R. Alfano Editor (Academic, Orlando, FL, 1984), Vol. II, p. 23.
[30] Y.-C. Chen, N. R. Raravikar, L. S. Schadler, P. M. Ajayan, Y.-P. Zhao, T.-M. Lu, G.-C. Wang, and X.-C. Zhang, Appl. Phys. Lett. **81**, 975 (2002).
[31] Z. V. Vardeny, J. Strait, D. Pfost, J. Tauc, and B. Abeles, Phys. Rev. Lett. **48**, 1132 (1982).
[32] J. J. Choi, X. Yang, Z. M. Norman, S. J. L. Billinge, and J. S. Owen, Nano Lett. **14**, 127 (2014).
[33] Q. Chen, H. Zhou, Z. Hong, S. Luo, H.-S. Duan, H.-H. Wang, Y. Liu, G. Li, and Y. Yang, J. Am. Chem. Soc. **136**, 622 (2014).
[34] S. D. Wolf, J. Holovsky, S.-J. Moon, P. Löper, B. Niesen, M. Ledinsky, F.-J. Haug, J.-H. Yum, and C. Ballif, J. Phys. Chem. Lett. **5**, 1035 (2014).
[35] S. Schmitt-Rink, D. S. Chemla, and D. A. B. Miller, Phys. Rev. B **32**, 6601 (1985).
[36] L. Lüer, S. Hoseinkhani, D. Polli, J. Crochet, T. Hertel, and G. Lanzani, Nat. Phys. **5**, 54 (2009).

Figure captions:

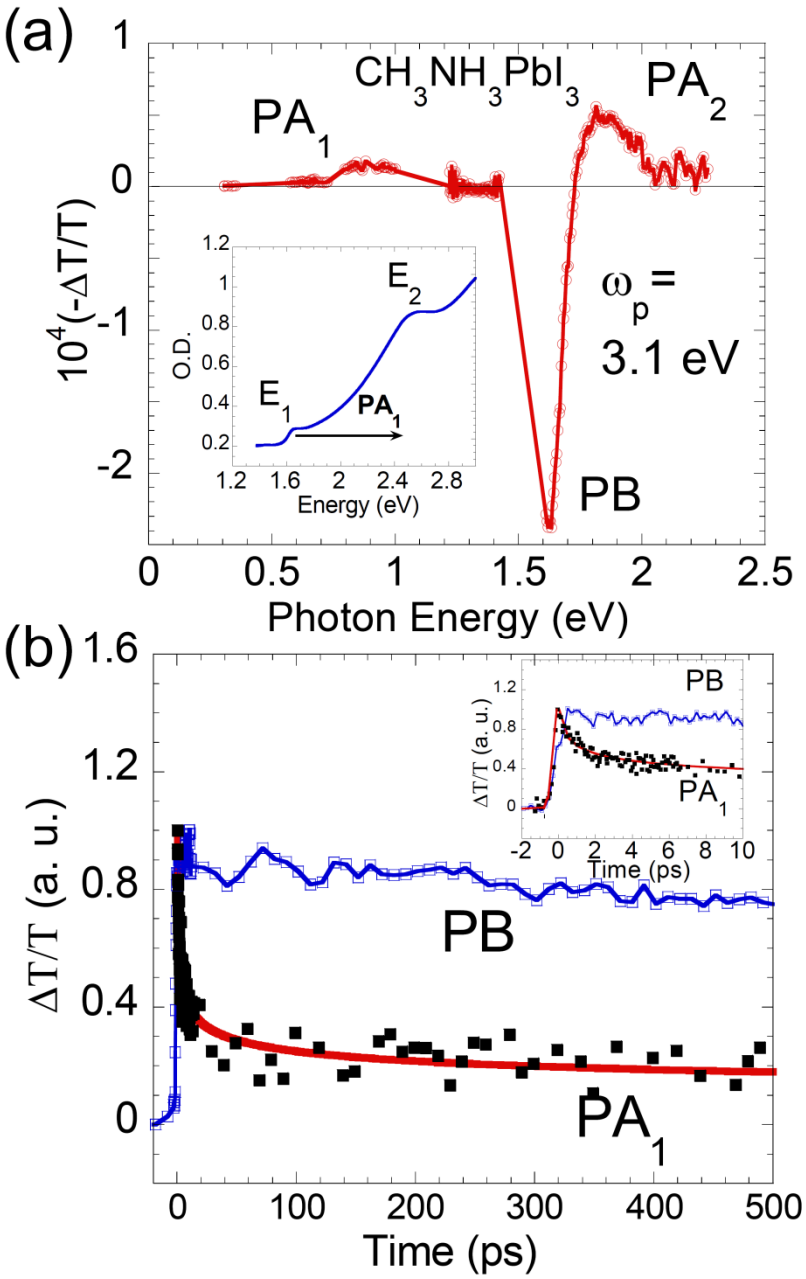

Figure 1(color online): Photomodulation (PM) spectroscopy of $CH_3NH_3PbI_3$ film excited at 400 nm at ambient. (a) Transient PM spectrum measured at t = 0; various bands are assigned. The inset shows the film absorption spectrum, where two excitons, namely E_1 and E_2 and the PA_1 transition are assigned. (b) Decay dynamics of PB and PA_1 bands up 500 ps and 10 ps (inset), respectively. The red line through the data points is a fit using a power law decay $(t/t_0)^{-\alpha}$, with α=0.21.

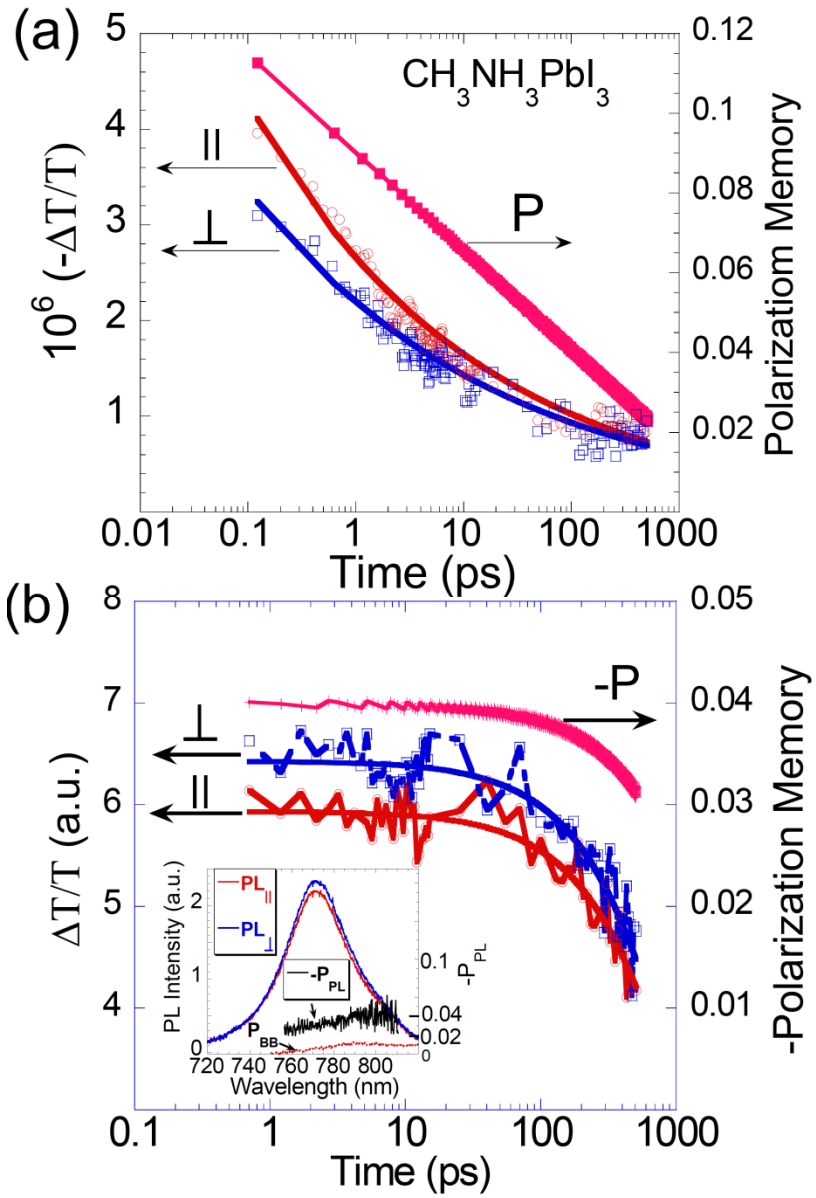

Figure 2(color online): Polarization memory (POM) dynamics of $CH_3NH_3PbI_3$ film excited at 400 nm. (a) and(b): Transient polarized response of PA_1(a) and PB(b) bands, where $\Delta T_{\parallel}$, $\Delta T_{\perp}$, and POM(t) decays are shown. The red and blue lines through the data points in (a) are fittings using power low decay $(t/t_0)^{-\alpha}$ with α=0.207 and α=0.186 for $\Delta T_{\parallel}$(t) (red)and $\Delta T_{\perp}$(t) (blue), respectively. The POM(t) response was calculated using the fits (see text). The inset in (b) shows the parallel ($PL_{\parallel}$) and perpendicular ($PL_{\perp}$) components of the PL emission spectrum respect to the pump polarization spectrum in $CH_3NH_3PbI_3$. The spectrum of the PL polarization degree, P_{PL}(see text) is also shown.

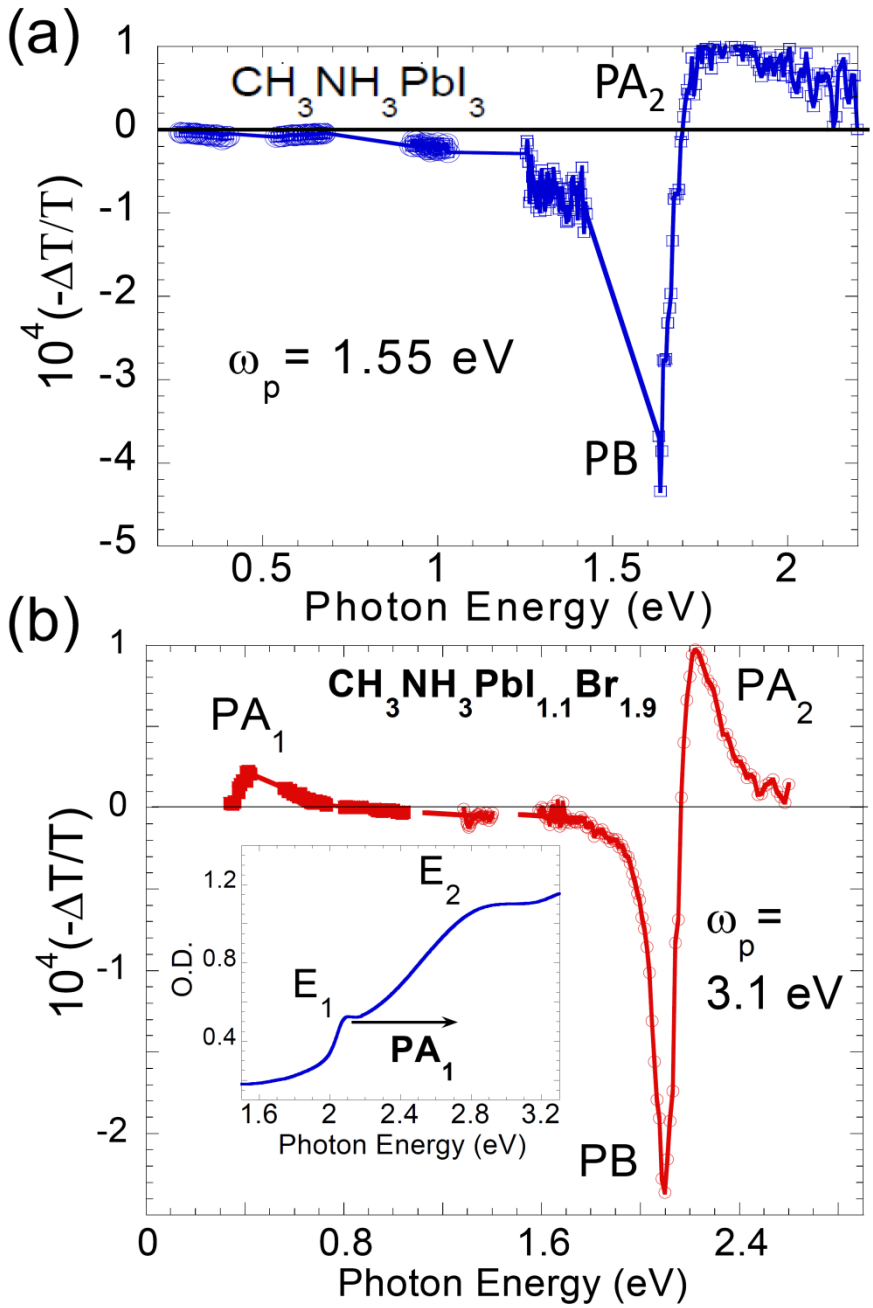

Figure 3(color online): (a) The photomodulation spectrum of $CH_3NH_3PbI_3$ film at t = 0 excited below-gap (800 nm), where various bands are assigned. (b) The photomodulation spectrum of $MAPbI_{1.1}Br_{1.9}$film at t = 0 excited at 400 nm, where various bands are assigned. The inset in (b) shows the film absorption spectrum, where two excitons, E_1 and E_2 and the PA_1 transition are assigned